Springer

KSME

Journal of Mechanical Science and Technology 33 (1) (2019) 341~349
www.springerlink.com/content/1738-494x(Print)/1976-3824(Online)
DOI 10.1007/s12206-018-1236-z

Experimental investigation of cutting force, surface roughness and tool wear in high-speed dry milling of AISI 4340 steel †

Guangming Zheng[1,2,*], Xiang Cheng[1,2], Li Li[1,2], Rufeng Xu[1,2] and Yebing Tian[1,2]

[1]*School of Mechanical Engineering, Shandong University of Technology, Zibo 255000, China*
[2]*Institute for Advanced Manufacturing, Shandong University of Technology, Zibo 255000, China*

(Manuscript Received May 23, 2018; Revised July 18, 2018; Accepted August 4, 2018)

Abstract

The high-speed dry milling of AISI 4340 steel was carried out with a CVD Al_2O_3/TiCN coated carbide tool. The relationships between cutting force, surface roughness and cutting parameter were conducted, and the influence of tool wear on cutting force and surface roughness was also investigated. The wear mechanism of coated tool was revealed by SEM micrograph and EDS analysis. Due to the lower tool wear rate, the increase of cutting forces and surface roughness R_a was smaller at the initial wear stage and the steady wear stage, whereas the increase of cutting forces was improved suddenly when the flank wear was more than 0.25 mm. Additionally, the coated tool wear was mainly caused by adhesion, abrasion, oxidation and diffusion, accompanied with a little peeling and chipping. The research results are expected to provide optimum cutting parameters for high-efficiency machining of high-strength steel.

Keywords: Coated tool; Dry milling; Cutting force; Surface roughness; Tool wear

1. Introduction

High-strength steel was a typical aviation material (e.g. aircraft landing gear), which had high strength, high transverse plasticity, high toughness, high hardness and excellent anti-fatigue properties [1-3]. However, the development of modern application of high-strength steel was confronted with great challenge due to the high cutting force, severe tool wear and unstable surface integrity in the cutting process [1, 4]. The high-speed machining (HSM) significantly outperformed as the obvious choice for enhancement of productivity and reduction of specific energy consumption [5]. So a practicable scheme was to optimize the cutting parameters and reveal the tool wear mechanisms to achieve the high-quality machining of high-strength steel.

The influence of cutting parameters on cutting forces, surface roughness and tool wear exhibited different trends with different coatings in machining of AISI 4340 steel. For the PVD TiAlN coated tool and the CVD TiCN/Al_2O_3/TiN coated tool, the effect of cutting parameters on cutting force, surface roughness and tool life was investigated in turning of AISI 4340 steel [6-8]. The cutting force of the PVD coated tool was improved sharply when the flank wear beyond 0.15 mm, while the cutting force of the CVD coated tool was enhanced uniformly when the flank wear up-to 0.2 mm [6]. And, the cutting forces of the CVD coated carbide tool vary almost linearly with the feed rate and depth of cut [7]. It is also concluded that the minimum cutting forces, surface roughness and better tool life can be obtained by limiting the cutting speed at the lower feed rate and depth of cut and, with respect to response surface methodology (RSM) and the desirability function approach [8]. Additionally, the surface roughness and flank wear was statistically significant influenced by feed rate and cutting speed in dry hard turning of AISI 4340 steel with TiN/TiCN/Al_2O_3/TiN coated tool [9]. Especially in case of the increased cutting speed caused to the reduction of surface roughness, accompanied with high flank wear [9]. The cutting forces of the TiN/TiCN/Al_2O_3/ZrCN coated tool were slightly lower than that of the TiN/TiCN/Al_2O_3/TiN coated tool, which can be attributed to the higher wear rate in initial cutting period [10]. Based on the RSM and per full factorial design during turning of AISI 4340 steel with a multilayer CVD TiN/MT-TiCN/Al_2O_3 coated tool [11], the combination of the low feed rate, depth of cut and high cutting speed should be applied, in order to obtain the lower cutting force and surface roughness. Under the high speed and low feed rate, the multilayer TiN coated tool produced the lower surface roughness in turning of AISI 4340 steel [12]. However, it is also concluded that the surface roughness was minimum affected by the depth of cut [12].

The ceramic tools and CBN tools were also used to ma-

*Corresponding author. Tel.: +86 15966961938
E-mail address: zhengguangming@sdut.edu.cn
† Recommended by Associate Editor Wonkyun Lee
© KSME & Springer 2019

chine of high-strength steel at the different cutting conditions to study the cutting force, surface roughness and tool wear. According to the analysis of performing analysis of variance (ANOVA) technique, the surface roughness was observed to get more affected with feed rate, while cutting force has been observed to have more influenced with depth of cut followed by feed, in turning of AISI 4340 steel with TiC mixed alumina ceramic tools [13]. The finish turning of hardened steel with ceramic tools was also carried out, and it is found that the depth of cut has less significant effect on tool wear and surface roughness [14]. The model of cutting force and surface roughness was also built in turning of AISI 52100 steel with ceramic tools [15]. It is proved that the depth of cut was the main parameter affecting the force components, and the best surface roughness was obtained by using small feed rate and large nose radius [15]. Furthermore, the Pearson's *r* correlation coefficient was used to analysis the influence of the tool wear on the surface roughness in the turning process of AISI H13 with ceramic tools, which proved no clear trend of the surface roughness depending on the tool wear [16]. On the other hand, the effects of cutting conditions on surface roughness and cutting forces in hard turning of X38CrMoV5-1 were also investigated with CBN tool [17]. The surface roughness was mainly influenced by feed rate and cutting speed, while cutting force components was also maximum influenced by the depth of cut [17]. The hard turning of AISI 52100 steel with CBN tool was also analyzed to predict the cutting force, surface roughness and tool wear using the method of ANOVA and RSM [18]. It is also reported that the depth of cut exhibited maximum influence on cutting forces, whereas the feed rate and cutting speed strongly influenced the surface roughness and tool life.

Obviously, the coated carbide tool was the most widely used, and turning process was selected mostly, during HSM of high-strength steel. In the application of the high-strength steel parts, there were also requirements for machining of plane or curved surface. Thus, the coated carbide tool with Al_2O_3/TiCN coating was used for high-speed dry milling of AISI 4340 steel in this work, to investigate the influence of milling parameters on cutting force, surface roughness and tool wear, and the influence of flank wear on cutting force and surface roughness. The research results are expected to provide optimum cutting parameters for high-speed and high-quality machining of high-strength steel.

2. Materials and methods

2.1 Workpiece material

The workpiece material was a type of high-strength alloy steel with martensitic structure, called AISI 4340. This material was provided by Dongguan Chang'an Huaming Die Steel Business Department (China). The standard heat treatment was also conducted by the manufacturer. The size of the workpiece was length (100 mm) × width (100 mm) × height (75 mm), which was processed by wire-electrical discharge machining. Tables 1 and 2 exhibit the main chemical compositions and the physical and mechanical properties of AISI 4340 steel, respectively, which were provided by the manufacturer. And the the physical and mechanical properties were obtained at room temperature after standard heat treatment. Additionally, the hardness of 43±1 HRC was obtained by a digital display Rockwell hardness tester (Model 200HRS-150), which was the average value of five measurements. The indentation load was 49 N and the holding time was 10 s.

Table 1. Main chemical composition of AISI 4340 steel.

Elements	wt.%	Elements	wt.%
C	0.40	Si	0.15
Mn	0.65	Cr	0.72
P	0.01	Mo	0.22
S	0.01	Ni	1.65

Table 2. Physical and mechanical properties of AISI 4340 steel.

Properties	Value	Properties	Value
Tensile strength (MPa)	1462	Elongation (%)	12
Yield strength (MPa)	1379	Reduction in area (%)	55

2.2 Tool material

A CVD coated tool with a surface layer of Al_2O_3 and a bottom layer of TiCN was used in the experiments, and its matrix was cemented carbide with high content of Co. The co-based matrix material had a good balance between the tool toughness and the deformation resistance. This coated insert was manufactured by Sumitomo (Japan), and its type was AXMT 123508PEER-G. The type of the end milling holder with three teeth was WEX 2020E, and its diameter was 20 mm.

2.3 Experimental method

The orthogonal experiment scheme with four factors and four levels was selected in this work to investigate the cutting forces, surface roughness and tool wear. The experimental design of high-speed dry milling of AISI 4340 steel is presented in Fig. 1. The milling experiments were carried out in the condition of down milling, accompanied with dry cutting condition. In the milling process, the cutting efficiency and cutting stability can be reduced if one insert was involved in cutting. However, this methodology can save the cost of cutting inserts and avoided the interference between inserts. Based on the purpose of this work, only one insert was used in the milling process. According to the author's research on high-speed turning of high-strength steel [19-21], and referring to the initial cutting parameters recommended by the manufacturing company of this tool, the range of the milling parameters in this work was determined as cutting speed v_c = 300 ~ 450 m/min, feed per tooth f_z = 0.02 ~ 0.0.8 mm/z, axial depth of cut a_p = 0.2 ~ 0.8 mm, radial depth of cut a_e = 1~ 4 mm.

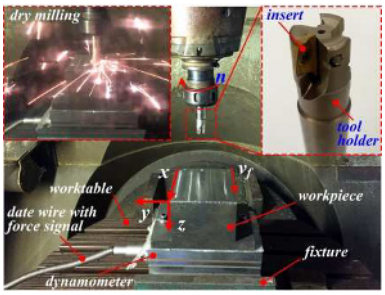

Fig. 1. Experimental design of high-speed dry milling of AISI 4340 steel.

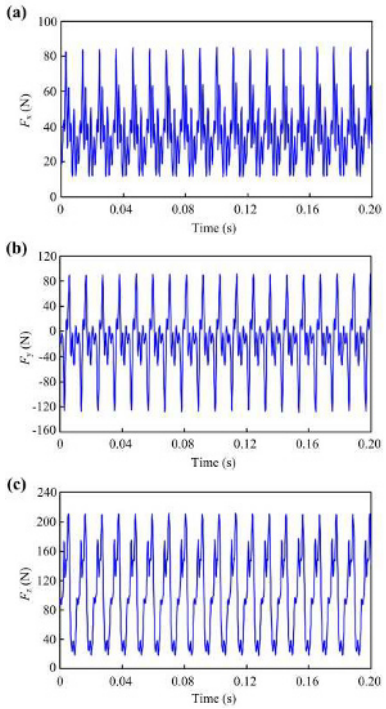

Fig. 2. Force signals in three directions at v_c = 350 m/min, f_z = 0.03 mm/z, a_p = 0.4 mm and a_e = 1 mm: (a) F_x; (b) F_y; (c) F_z.

2.4 Experimental equipment

As can be seen from Fig. 1, the high-speed milling experiment was carried out on the five axis CNC machining center DMU 70 eVolution with the maximum spindle speed of 18000 r/min. The cutting force was measured by the piezoelectric three direction cutting force measurement system with the model of KISTLER 9257B, while the machined surface roughness of AISI 4340 steel was measured by a portable surface roughness tester with the model of CS-3200. The force signals in three directions and the chart of surface roughness are exhibited in Figs. 2 and 3, respectively. Table 3 expressed the experimental results for cutting force (F_x, F_y, F_z) and surface roughness (R_a).

Tool wear values were measured at various stages of each test with a digital toolmaker's microscope (Model USB200, China) dismounting the inserts from the tool holder. Scanning electron microscope (SEM, Model Quanta 250) was employed to observe worn surfaces produced by various wear mechanisms. And the elemental compositions of wear products were evaluated by energy-dispersive X-ray spectroscopy (EDS). A cutting tool was rejected and further machining stopped based on the combination of rejection criteria: average flank wear VB ≥ 0.30 mm.

Table 3. Experimental results for cutting force in three directions F_x, F_y, F_z (N) and surface roughness R_a (μm).

No	a_p	v_c	f_z	a_e	F_x	F_y	F_z	R_a
1	0.2	250	0.03	2	16	11	88	0.41
2	0.2	350	0.06	3	18	25	94	0.42
3	0.2	450	0.09	4	17	35	106	0.49
4	0.2	550	0.12	1	27	43	94	0.56
5	0.4	250	0.06	4	31	35	136	0.40
6	0.4	350	0.03	1	44	34	99	0.43
7	0.4	450	0.12	2	50	47	162	0.68
8	0.4	550	0.09	3	60	44	181	0.51
9	0.6	250	0.09	1	46	79	363	0.40
10	0.6	350	0.12	4	80	66	443	0.56
11	0.6	450	0.03	3	97	33	499	0.31
12	0.6	550	0.06	2	56	59	147	0.50
13	0.8	250	0.12	3	134	157	713	0.53
14	0.8	350	0.09	2	134	172	560	0.63
15	0.8	450	0.06	1	131	158	357	0.37
16	0.8	550	0.03	4	153	154	1054	0.58

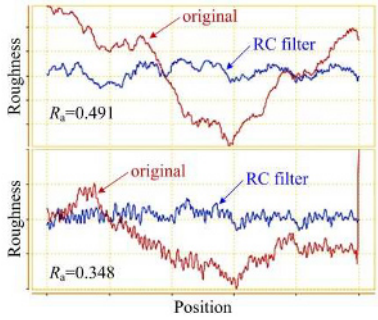

Fig. 3. Chart of surface roughness.

3. Results and discussion

3.1 ANORA and ANOVA

As can be seen from Fig. 2, the three component forces varied periodically, which can be mainly attributable to the changes of cutting thickness in cut-in and cut-out process. Furthermore, the maximum peak value of the three component forces was in *z* direction, which was the chief component. It also can be seen that the fluctuation of cutting force was very large in a cycle of cut-in and cut-out. In order to ensure the uniformity of experimental data, the peak of the cutting force was selected to research. In Table 3, the value of the cutting force and the surface roughness was the average peak of the

cutting force and the average surface roughness, in the initial cutting stage, respectively.

The analysis of range (ANORA) method was applied to analyze the three component forces and surface roughness. Table 4 show the ANORA results for cutting forces and surface roughness, from which it can be seen that the most important factor for F_x was a_p, followed by f_z and v_c, and finally a_e, while the most important factor for F_y and F_z was also a_p, followed by f_z and a_e, and finally v_c. Therefore, it was particularly required to control a_p during dry milling of AISI 4340 steel for reducing cutting force. In order to ensure no decrease of cutting efficiency, a combination of small a_p and high a_e can lead to a lower F_x, compared with the combination of small a_p and high v_c for F_y and F_z. On the other hand, the most important factor for R_a was f_z, followed by a_e and v_c, and finally a_p. The small f_z and high a_p was the best combination to achieve the lower surface roughness R_a, as can be seen from Table 4.

The ANOVA method was also used to quantitatively analyze the experimental results, with the objective of analyzing the effect of milling parameters on the component forces and surface roughness. The results of the ANOVA with the response measurements (cutting forces and surface roughness) are shown in Tables 5-8. The tables expressed the source of variation (SV), sum of squares (SS), degrees of freedom (DF), mean square (MS), F-value (F) and P-value (P). A low P (≤ 0.05) indicated statistical significance for the source on the corresponding response, that is to say, this analysis was carried out for a confidence of 95 %. As can be seen from Tables 5-8, the axial depth of cut a_p had the greatest influence on cutting force component F_x, F_y, F_z, while the feed per tooth f_z had the greatest influence on surface roughness R_a. Therefore, the results of ANOVA were consistent with that of ANORA.

Table 4. ANORA results for cutting forces and surface roughness.

Parameters		Influence order		
		High	Medium	Low
Cutting forces	F_x	a_p	f_z, v_c	a_e
	F_y	a_p	f_z, a_e	v_c
	F_z	a_p	f_z, a_e	v_c
Surface roughness	R_a	f_z	a_e, v_c	a_p

Table 5. Analysis of variance for F_x.

SV	SS	DF	MS	F	P
a_p	30788.409	3	10262.803	126.767	0.001
v_c	773.744	3	257.915	3.186	0.183
f_z	828.294	3	276.098	3.410	0.170
a_e	559.875	3	186.625	2.305	0.255
Error	242.874	3	80.958		
Total	33193.196	15			

Table 6. Analysis of variance for F_y.

SV	SS	DF	MS	F	P
a_p	43511.985	3	14503.995	452.842	<0.001
v_c	126.590	3	42.197	1.317	0.413
f_z	1428.910	3	476.303	14.871	0.026
a_e	381.974	3	127.325	3.975	0.143
Error	96.087	3	32.029		
Total	45545.547	15			

Table 7. Analysis of variance for F_z.

SV	SS	DF	MS	F	P
a_p	824268.669	3	274756.223	13.481	0.030
v_c	17523.701	3	5841.234	0.287	0.834
f_z	133225.118	3	44408.373	2.179	0.269
a_e	123407.244	3	41135.748	2.018	0.289
Error	61143.827	3	20381.276		
Total	1159568.558	15			

Table 8. Analysis of variance for R_a.

SV	SS	DF	MS	F	P
a_p	0.017	3	0.006	2.535	0.232
v_c	0.025	3	0.008	3.646	0.158
f_z	0.070	3	0.023	10.224	0.044
a_e	0.036	3	0.012	5.262	0.103
Error	0.007	3	0.002		
Total	0.156	15			

3.2 Empirical models of cutting force and surface roughness

In cutting process, the influence factors of cutting force and surface roughness had many source, such as tool (material, geometries), workpiece (material, machinability), machine (stability, power) and cutting conditions (cutting parameters, coolant and lubrication). Two methods of the simplicity mathematic model of AISI 4340 milling process for the experimental (measured) response (cutting force or surface roughness) in terms of the investigated independent variables were shown in the work.

3.2.1 Exponential model

The exponential model can be shown in the following form.

$$P = C \cdot a_p^{b1} \cdot v_c^{b2} \cdot f_z^{b3} \cdot a_e^{b4} \quad (1)$$

where P was the cutting force (N) or surface roughness (μm), a_p, v_c, f_z and a_e were axial depth of cut (mm), cutting speed (m/min), feed per tooth (mm/z) and radial depth of cut (mm), respectively.

The model parameters can be estimated using experimental data, taking natural logarithms converts the above non-linear model can be transformed into a first-order polynomial. And then the relationship can be presented as matrix. According to this exponential model and experimental results (Table 3), the cutting force components (F_x, F_y, F_z) and surface roughness

(R_a) can be described as follow.

$$F_x = 10.4354 \cdot a_p^{1.3447} \cdot v_c^{0.4655} \cdot f_z^{0.0283} \cdot a_e^{0.0345} \quad (2)$$

$$F_y = 68.3158 \cdot a_p^{1.1911} \cdot v_c^{0.3531} \cdot f_z^{0.4680} \cdot a_e^{-0.1035} \quad (3)$$

$$F_z = 665.7833 \cdot a_p^{1.3363} \cdot v_c^{-0.0247} \cdot f_z^{0.0399} \cdot a_e^{0.3491} \quad (4)$$

$$R_a = 0.2796 \cdot a_p^{0.0344} \cdot v_c^{0.1897} \cdot f_z^{0.2262} \cdot a_e^{0.0565}. \quad (5)$$

As can be described in Eq. (4), a_p had a significant influence on the chief component F_z and f_z and v_c had a very small effect. Additionally, R_a was greatly affected by f_z, followed by v_c, a_e and a_p, which is described in Eq. (5).

3.2.2 Polynomial model

The second order polynomial model can be shown in the following form [22, 23].

$$y = b_0 + \sum_{i=1}^{n} b_i x_i + \sum_{i=1}^{n} b_{ii} x_i^2 + \sum_{i<j}^{n} b_{ij} x_i x_j + \varepsilon \quad (6)$$

where b_0 was the free term of the regression equation, the coefficients, b_1, b_2, … b_n and b_{11}, b_{22}, … b_{nn} were the linear and the quadratic terms, respectively; while b_{12}, b_{13}, … b_{1n}, b_{23}, … , $b_{(n-1)n}$ were the interacting terms. In this work, $n = 4$, x_1, x_2, x_3, x_4 was a_p, v_c, f_z and a_e, respectively. y was the cutting force (N) or surface roughness (μm). ε was experimental error, which can be ignored.

The parameters of b_0, b_i, b_{ii}, b_{ij} can be estimated using the measured data of cutting forces and surface roughness in Table 3. So the polynomial formula of cutting force and surface roughness can be described as follow.

$$\begin{aligned} F_x = {} & -41.4741 - 19.1685 \cdot a_p + 0.1888 \cdot v_c - 521.1837 \cdot f_z + \\ & 27.8293 \cdot a_e + 196.5603 \cdot a_p^2 + 0.0001 \cdot v_c^2 + 1080.7512 \cdot f_z^2 - \\ & 3.4167 \cdot a_e^2 - 0.0336 \cdot a_p \cdot v_c - 367.3747 \cdot a_p \cdot f_z + 4.2067 \cdot a_p \cdot a_e + \\ & 0.0354 \cdot v_c \cdot f_z - 0.0223 \cdot v_c \cdot a_e + 22.0822 \cdot f_z \cdot a_e \end{aligned} \quad (7)$$

$$\begin{aligned} F_y = {} & 116.0564 - 389.2414 \cdot a_p - 0.0733 \cdot v_c 1214.1391 \cdot f_z - \\ & 42.4797 \cdot a_e + 565.6888 \cdot a_p^2 - 0.0003 \cdot v_c^2 - 11742.2644 \cdot f_z^2 + \\ & 4.7340 \cdot a_e^2 - 0.0015 \cdot a_p \cdot v_c - 705.9569 \cdot a_p \cdot f_z + 24.5489 \cdot a_p \cdot a_e + \\ & 2.2386 \cdot v_c \cdot f_z + 0.0311 \cdot v_c \cdot a_e - 27.8138 \cdot f_z \cdot a_e \end{aligned} \quad (8)$$

$$\begin{aligned} F_z = {} & 314.4214 - 613.7155 \cdot a_p + 0.5713 \cdot v_c - 1330.5647 \cdot f_z - \\ & 204.2613_4 \cdot a_e + 1332.9517 \cdot a_p^2 - 0.0019 \cdot v_c^2 + 33888.9250 \cdot f_z^2 + \\ & 23.7406 \cdot a_e^2 - 1.0414 \cdot a_p \cdot v_c - 1043.0400 \cdot a_p \cdot f_z + 185.7412 \cdot a_p \cdot a_e - \\ & 2.1514 \cdot v_c \cdot f_z + 0.5235 \cdot v_c \cdot a_e - 1684.0529 \cdot f_z \cdot a_e \end{aligned} \quad (9)$$

$$\begin{aligned} R_a = {} & 0.6927 - 1.2467 \cdot a_p - 0.0002 \cdot v_c + 8.5035 \cdot f_z - 0.1251 \cdot a_e + \\ & 0.4461 \cdot a_p^2 - 54.3180 \cdot f_z^2 - 0.0229 \cdot a_e^2 + 0.0016 \cdot a_p \cdot v_c - \\ & 9.4889 \cdot a_p \cdot f_z + 0.3092 \cdot a_p \cdot a_e + 0.0094 \cdot v_c \cdot f_z + \\ & 0.0002 \cdot v_c \cdot a_e + 0.5359 \cdot f_z \cdot a_e . \end{aligned} \quad (10)$$

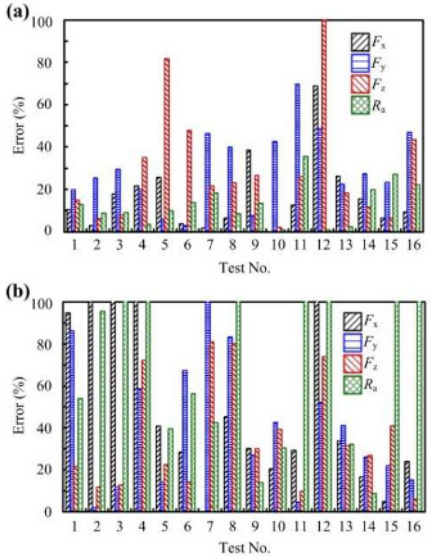

Fig. 4. Error between the calculated values and the experimental values: (a) Exponential model; (b) polynomial model.

The calculated values of F_x, F_y, F_z and R_a obtained from Eqs. (3)-(5) and (7)-(10), were compared with the experimental values got from Table 3. Fig. 4 shows the error between the calculated values and the experimental values, including exponential model and polynomial model.

For the exponential model, the average error of F_x, F_y, F_z and R_a value was 16.73 %, 29.87 %, 31.01 %, 12.91 %, respectively. As can be seen in Fig. 4(a), the biggest error of F_x value was 68.65 % in test No. 12, followed by 38.50 % in test No. 9, and the error of the other tests was less than 30 %. The biggest error of F_y value was 69.72 % in test No. 11, and the error of the other tests was less than 50 %. For the error value of F_z, there were two sets of errors more than 50 %, including test No. 5 and test No. 12. The biggest error of R_a value was 35.50 % in test No. 11, followed by 27.14 % in test No. 15 and 22.12 % in test No. 16, and the error of the other tests was less than 20 %.

For the polynomial model, however, the average error of F_x, F_y, F_z and R_a value was 57.84 %, 41.33 %, 35.70 %, 81.22 %, respectively, which was very higher than that of the exponential model. Therefore, the polynomial model did not apply to the prediction of cutting force and surface roughness in high-speed milling of high-strength steel.

Based on the ANORA, ANOVA and empirical models, it can be concluded that the combined cutting parameters of a_p = 0.2 ~ 0.4 mm, f_z = 0.03 ~ 0.06 mm/z, v_c = 350 ~ 450 m/min, a_e = 3 ~ 4 mm were recommended for the low cutting forces and surface roughness, during the high-speed dry milling of AISI 4340 with Al_2O_3/TiCN coated tool.

3.3 Influence of tool wear on cutting force and surface roughness

The average peak values of the force signals achieved by

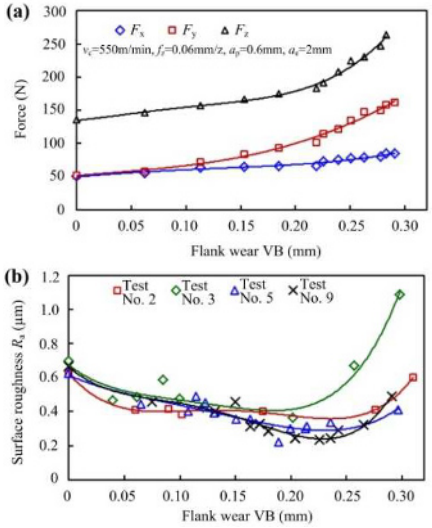

Fig. 5. Changes of (a) cutting force in three directions; (b) surface roughness R_a with flank wear VB.

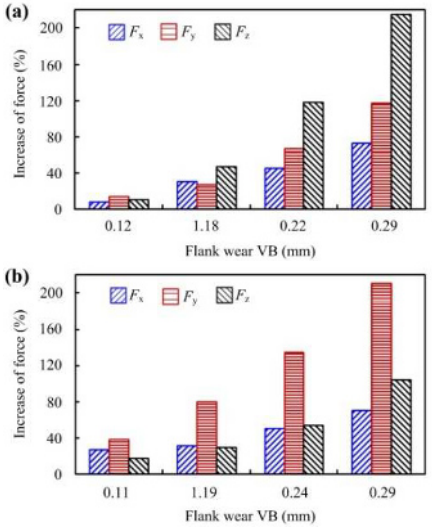

Fig. 6. Increase of cutting force with flank wear VB: (a) v_c = 350 m/min, f_z = 0.03 mm/z, a_p = 0.4 mm, a_e = 1 mm; (b) v_c = 550 m/min, f_z = 0.06 mm/z, a_p = 0.6 mm, a_e = 2 mm.

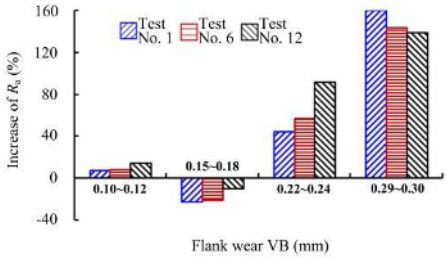

Fig. 7. Increase of surface roughness R_a with flank wear VB.

the dynamometer and the average value of the surface roughness R_a achieved by the roughness tester in three measurements were used to analyze the influence of tool wear on cutting force and surface roughness. Fig. 5(a) depicts the changes of cutting force components with the progress in flank wear VB at v_c = 550 m/min, f_z = 0.06 mm/z, a_p = 0.6 mm, a_e = 2 mm. As can be seen from Fig. 5(a), the cutting force in X direction F_x was basically unchanged with the increase of flank wear. It is indicated that the influence of flank wear on F_x was very small. At the initial wear stage and the steady wear stage of the coated tool, the changes of F_y and F_z was also very small. When the flank wear was more than 0.2 mm, however, the increase of F_y and F_z was accelerated significantly.

Fig. 5(b) exhibits the changes of surface roughness R_a with the progress in flank wear VB at tests Nos. 2, 3, 5 and 9. The initial surface roughness R_a was controlled in 0.6~0.8 μm in each test to avoid the influence of different initial surface roughness. As can be seen from Fig. 5(b), during the steady wear stage of the coated tool, the surface roughness R_a was lower and relatively stable, which was about between 0.3 μm and 0.6 μm. It increased sharply when the flank wear VB was beyond 0.25 mm. In particularly, the surface roughness R_a improved suddenly at the sharp wear stage in test No. 3 (v_c = 450 m/min, f_z = 0.09 mm/z, a_p = 0.2 mm and a_e = 4).

To characterize the inter-relationship between cutting force and flank wear, the increase of cutting force with flank wear was also investigated, which is shown in Fig. 6. At the initial wear stage and the steady wear stage of the coated tool, the increase of cutting forces was smaller due to the lower tool wear rate. However, the cutting forces of F_x, F_y and F_z were improved suddenly when the flank wear was more than 0.25 mm, approximately by 73 %, 117 % and 214 % at v_c = 350 m/min, respectively, and that were improved approximately by 70 %, 210 % and 104 % at v_c = 550 m/min, respectively.

As can be seen from Fig. 6, the increase of F_x was minimal in the three component forces, which was enhanced from 8 % (VB = 0.12 mm) to 73 % (VB = 0.29 mm) at v_c = 350 m/min and from 27 % (VB = 0.11 mm) to 70 % (VB = 0.29 mm) at v_c = 550 m/min. For F_z, the increase of cutting force (%) was the highest in three components when the flank wear beyond 1.18 mm at v_c = 350 m/min (Fig. 6(a)), which was improved from 47 % (VB = 1.18 mm) to 214 % (VB = 0.29 mm). However, at v_c = 550 m/min (Fig. 6(b)), the component with the highest increase was F_y, and the increase of cutting force was from 37 % (VB = 0.11) to 210 % (VB = 0.29).

The increase of surface roughness R_a with flank wear VB is presented in Fig. 7, from which it can be seen that the increase of surface roughness R_a was also very low at the initial wear stage and the steady wear stage of the coated tool, because of the sharp cutting edge and low flank wear. Especially, the negative growth of surface roughness was found in the flank wear of 0.15 mm~0.18 mm, which indicated that the high surface quality can be obtained after the cutting process into stable stage. It also can be seen that beyond a flank wear of 0.25 mm, the surface roughness R_a was increased suddenly at test Nos. 1, 6 and 12, due to high tool wear, nearly 160 %, 143 % and 138 %, respectively.

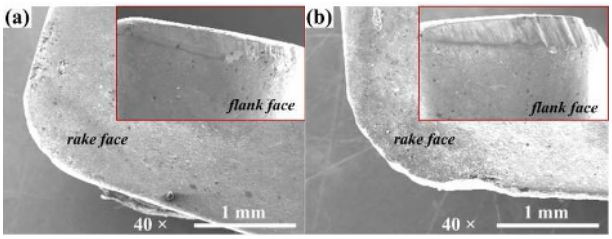

Fig. 8. Wear morphology of the Al_2O_3/TiCN coated tool: (a) v_c = 350 m/min, f_z = 0.03 mm/z, a_p = 0.4 mm, a_e = 1 mm; (b) v_c = 550 m/min, f_z = 0.06 mm/z, a_p = 0.6 mm, a_e = 2 mm.

3.4 Wear mechanical of the coated tool in high-speed milling of AISI 4340

Fig. 8 shows the wear morphology of the Al_2O_3/TiCN coated tool, from which it can be seen that the tool wear were presented on both rake and flank face, but the flank wear was more serious. As can be seen from rake wear, the abnormal wear patterns of peeling off (Fig. 8(a)) and chipping (Fig. 8(b)) were appeared. On the flank face, the tool wear band was even at the two different cutting parameters, which can explain the reason for adopting the average flank wear band VB ≥ 0.30 mm as a rejection criterion in this work.

Fig. 9 exhibits the SEM micrograph of tool wear at v_c = 350 m/min, f_z = 0.03 mm/z, a_p = 0.4 mm and a_e = 1 mm. Fig. 10 exhibits the EDS analysis results of areas 1-3 in Fig. 9. Adhesion was the main cause of tool wear on the rake face (Fig. 9(a)), especially near the cutting edge. And micro-chipping was also found in Fig. 9(a). As can be seen in Fig. 10(a), a large amount of coating elements (e.g. Al, O, Ti, N, C) and a small amount of workpiece elements (e.g. Fe, Ni, Mn) were detected in area 1 which was away from the cutting edge. However, a sharp increase in the content of Fe element was found in area 2 which was close to the cutting edge, as can be seen in Fig. 10(b). On the one hand, it is proved that the adhesion was very serious near the cutting edge. On the other hand, the element diffusion may occur and the iron oxide was possible formed under the action of high stress and high cutting temperature, which can result in diffusion wear and oxidation wear.

As can be seen on the flank wear micrograph in Figs. 9(b) and (d), the marks of abrasive wear were clearly presented, beside severe adhesive wear. According to the EDS analysis results of area 3 (Fig. 10(c)), a low content of Al and a high content of O were presented, which indicted the wear out of the surface coating Al_2O_3 and the enhanced possibility of oxidation wear. Furthermore, both titanium oxide and iron oxide can be formed under the condition of high temperature and high pressure in the milling process, due to the chemical reaction between the high content O and the bottom coating and workpiece elements. The former can reduce friction coefficient and be beneficial for milling process, whereas the latter can reduce the surface hardness of the coated tool and then aggravate tool wear. Thus, the coated tool flank wear was mainly caused by adhesion, hard particles, element diffusion and oxidation.

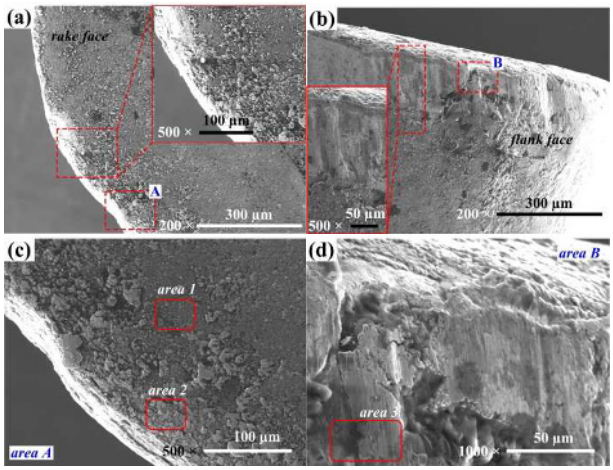

Fig. 9. SEM micrograph of tool wear at v_c = 350 m/min, f_z = 0.03 mm/z, a_p = 0.4 mm and a_e = 1 mm: (a) Rake face; (b) flank face; (c) area A; (d) area B.

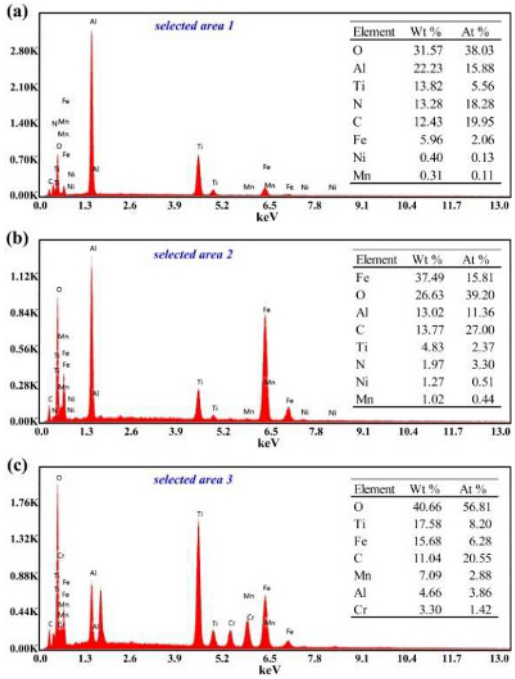

Fig. 10. EDS analysis results of (a) Area 1; (b) area 2; (3) area 3 in Fig. 9.

Fig. 11 shows the SEM micrograph of tool wear at v_c = 550 m/min, f_z = 0.06 mm/z, a_p = 0.6 mm and a_e = 2 mm, from which it can be seen that both the probability of brittle failure (e.g. chipping) and the bulk adhesion metal material were enhanced with the increase of the cutting parameters. Moreover, the adhesive wear and chipping were also the main wear mechanical on rake face (Fig. 11(a)). On the flank face, the adhesion band near the cutting edge was widened significantly, and the strips of groove became more and deeper. So the adhesive wear and abrasive wear were extremely serious at higher cutting parameters.

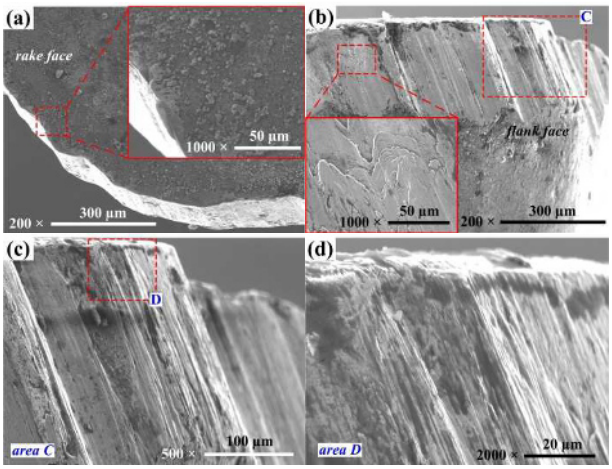

Fig. 11. SEM micrograph of tool wear at v_c = 550 m/min, f_z = 0.06 mm/z, a_p = 0.6 mm and a_e = 2 mm: (a) Rake face; (b) flank face; (c) area C; (d) area D.

In a word, the normal wear of the coated tool was main failure mode in the high-speed milling of high-strength steel. This work also had industrial applications, such as automotive, aerospace and power industries, because of the excellent properties of the high-strength steel. Through this research, we can optimize the cutting parameters and reveal failure mechanism to achieve the high-efficiency and high-quality machining of high-strength steel.

4. Conclusions

(1) According to ANORA and ANOVA, a_p had the greatest influence on component force F_x, F_y, F_z, while f_z had the greatest influence on R_a, in the high-speed dry milling of AISI 4340 with Al_2O_3/TiCN coated tool.

(2) In order to reduce cutting forces and surface roughness, the combined cutting parameters of a_p = 0.2 ~ 0.4 mm, f_z = 0.03 ~ 0.06 mm/z, v_c = 350 ~ 450 m/min, a_e = 3 ~ 4 mm were recommended by the empirical models.

(3) In the initial wear stage and the steady wear stage, the increase of cutting forces (F_x, F_y, F_z) and R_a were smaller, because of the lower tool wear. Especially, the negative growth of R_a was found in the flank wear of 0.15 mm ~ 0.18 mm. However, the cutting forces were improved suddenly when the flank wear was more than 0.25 mm.

(4) Based on the analysis of worn morphology and elements in the high-speed dry milling of AISI 4340, the main wear mechanical of the Al_2O_3/TiCN coated tool involved adhesive wear, abrasive wear, oxidation wear and diffusion wear, accompanied with an abnormal wear of chipping and peeling off.

Acknowledgments

This work was supported by the National Natural Science Foundation of China (51505264), the Zibo City - Shandong University of Technology Cooperative Projects (2017ZBXC032), and the Youth Teacher Development Support Program of Shandong University of Technology.

References

[1] Q. Xu, J. Zhao and X. Ai, Fabrication and cutting performance of Ti(C,N)-based cermet tools used for machining of high-strength steels, *Ceram. Int.*, 43 (2017) 6286-6294.

[2] D. Wang, J. Zhao, Y. Cao, C. Xue and Y. Bai, Wear behavior of an Al_2O_3/TiC/TiN micro-nano-composite ceramic cutting tool in high-speed turning of ultra-high-strength steel 300 M, *Int. J. Adv. Manuf .Technol.*, 87 (2016) 3301-3306.

[3] M. Hadhri, A. E. Ouafi and N. Barka, Prediction of the hardness profile of an AISI 4340 steel cylinder heat-treated by laser - 3D and artificial neural networks modelling and experimental validation, *J. Mech. Sci. Technol.*, 31 (2) (2017) 615-623.

[4] S. Kumar, D. Singh and N. S. Kalsi, Analysis of surface roughness during machining of hardened AISI 4340 steel using minimum quantity lubrication, *Mater. Today Proc.*, 4 (2017) 3627-3635.

[5] K. A. Al-Ghamdi and A. Iqbal, A sustainability comparison between conventional and high-speed machining, *J. Clean. Prod.*, 108 (2015) 192-206.

[6] S. Chinchanikar and S. K. Choudhury, Characteristic of wear, force and their inter-relationship: In-process monitoring of tool within different phases of the tool life, *Procedia Mater. Sci.*, 5 (2014) 1424-1433.

[7] S. Chinchanikar and S. K. Choudhury, Investigations on machinability aspects of hardened AISI 4340 steel at different levels of hardness using coated carbide tools, *Int. J. Refract. Met. Hard Mater.*, 38 (2013) 124-133.

[8] S. Chinchanikar and S. K. Choudhury, Effect of work material hardness and cutting parameters on performance of coated carbide tool when turning hardened steel: An optimization approach, *Measurement*, 46 (2013) 1572-1584.

[9] S. R. Das, A. Panda and D. Dhupal, Experimental investigation of surface roughness, flank wear, chip morphology and cost estimation during machining of hardened AISI 4340 steel with coated carbide insert, *Mech. Adv. Mater. Mod. Process.* (2017) 3: 9.

[10] A. K. Sahoo and B. Sahoo, Experimental investigations on machinability aspects in finish hard turning of AISI 4340 steel using uncoated and multilayer coated carbide inserts, *Measurement*, 45 (2012) 2153-2165.

[11] R. Suresh, S. Basavarajappa and V. N. Gaitonde, Samuel GL, Machinability investigations on hardened AISI 4340 steel using coated carbide insert, *Int. J. Refract. Met. Hard Mater.*, 33 (2012) 75-86.

[12] S. Sahu and B. B. Choudhury, Optimization of Surface Roughness using Taguchi methodology & prediction of tool wear in hard turning tools, *Mater. Today Proc.*, 2 (2015) 2615-2623.

[13] A. Pal, S. K. Choudhury and S. Chinchanikar, Machinability assessment through experimental investigation during

hard and soft turning of hardened steel, *Procedia Mater. Sci.*, 6 (2014) 80-91.

[14] S. Saini, I. S. Ahuja and V. S. Sharma, Influence of cutting parameters on tool wear and surface roughness in hard turning of AISI H11 tool steel using ceramic tools, *Int. J. Precis. Eng. Manuf.*, 13 (8) (2012) 1295-1302.

[15] I. Meddour, M. A. Yallese, R. Khattabi, M. Elbah and L. Boulanouar, Investigation and modeling of cutting forces and surface roughness when hard turning of AISI 52100 steel with mixed ceramic tool: Cutting conditions optimization, *Int. J. Adv. Manuf. Technol.*, 77 (2015) 1387-1399.

[16] R. Ferreira, J. Řehoř, C. H. Lauro, D. Carou and J. P. Davim, Analysis of the hard turning of AISI H13 steel with ceramic tools based on tool geometry: Surface roughness, tool wear and their relation, *J. Braz. Soc. Mech. Sci. Eng.*, 38 (2016) 2413-2420.

[17] H. Aouici, M. A. Yallese, A. Belbah, Mfameur and M. Elbah, Experimental investigation of cutting parameters influence on surface roughness and cutting forces in hard turning of X38CrMoV5-1 with CBN tool, *Sādhanā,* 38 (2013) 429-445.

[18] S. Khamel, N. Ouelaa and K. Bouacha, Analysis and prediction of tool wear, surface roughness and cutting forces in hard turning with CBN tool, *J. Mech. Sci. Technol.*, 26 (11) (2012) 3605-3616.

[19] G. Zheng, X. Cheng, X. Yang, R. Xu, J. Zhao and G. Zhao, Self-organization wear characteristics of MTCVD-TiCN-Al_2O_3 coated tool against 300M steel, *Ceram. Int.*, 43 (16) (2017) 13214-13223.

[20] G. Zheng, L. Li, Z. Li, J. Gao and Z. Niu, Wear mechanisms of coated tools in high-speed hard turning of high strength steel. *Int. J. Adv. Manuf. Technol.*, 94 (9-12) (2018) 4553-4563.

[21] G. Zheng, R. Xu, X. Cheng, G. Zhao, L. Li and J. Zhao, Effect of cutting parameters on wear behavior of coated tool and surface roughness in high-speed turning of 300M, *Measurement*, 125 (2018) 99-108.

[22] A. Bhattacharyya, *Metal cutting theory and practice*, New Central Book Agency (P) Ltd, Calcutta. (1998).

[23] A. V. M. Subramanian, M. D. G. Nachimuthu and V. Cinnasamy, Assessment of cutting force and surface roughness in LM6/SiC pusing response surface methodology, *J. Appl. Res. Technol.*, 15 (2017) 283-296.

Guangming Zheng is an Associate Professor at School of Mechanical Engineering, Shandong University of Technology, Zibo, China. He received his Ph.D. degree in 2012 from Shandong University, Jinan, China. His research interests include high-efficiency machining technology, manufacturing process of cutting tool, and surface integrity.